LAWRENCE
LIVERMORE
NATIONAL
LABORATORY

UCRL-TR-221110

Deep Ultrasound Enhancements Final Report

M. Quarry, G. Thomas, W. Ward, D. Gardner

May 1, 2006

This work was performed under the auspices of the U.S. Department of Energy by University of California, Lawrence Livermore National Laboratory under Contract W-7405-Eng-48.

Executive Summary

This study involves collaboration between Los Alamos National Laboratory and Lawrence Livermore National Laboratory to enhance and optimize LANL's ultrasonic inspection capabilities for production. Deep-penetrating ultrasonic testing enhancement studies will extend the current capabilities, which only look for disbonds. Current ultrasonic methods in production use 15-20 MHz to inspect for disbonds. The enhanced capabilities use 5 MHz to penetrate to the back surface and image the back surface for any flaws. The enhanced capabilities for back surface inspection use transducers and squirter modifications that can be incorporated into the existing production system. In a production setup the current 15-20 MHz transducer and squirter would perform a bond inspection, followed by a deep inspection that would be performed by simply swapping out the 5 MHz transducer and squirter.

Surrogate samples were manufactured of beryllium and bismuth to perform the ultrasonic enhancement studies. The samples were used to simulate flaws on the back surface and study ultrasound's ability to image them. The ultrasonic technique was optimized by performing experiments with these samples and analyzing transducer performance in detecting flaws in the surrogate. Beam patterns were also studied experimentally using a steel ball reflector to measure beam patterns, focal points, and sensitivities to better understand the relationship between design and performance. Many transducers were evaluated including transducers from LANL's production system, LLNL, and other commercially available transducers. Squirter design was also analyzed while performing experiments

Flat-bottom holes and ball-mill defects of various sizes were introduced into the samples for experimentation. Flaws depths were varied from .020" to 0.060", and diameters varied from 0.0625" to 0.187". The smallest defect, .020" depth and 0.0625", was detected. Ultrasonic amplitude features produced better images than time-of-flight features. 5 MHz was the optimal frequency, because it was able to penetrate deepest into the materials. Squirter standoff distance was found to be significant, and a standoff of an inch or so with an opening that is larger than the diameter of the transducer is recommended. Recommendations for enhancement are made based on the results of the experimental studies on Be-Bi samples.

Future work should focus on deployment of a deep ultrasound technology and obtain initial results with real units. Efforts should be made to develop a reference sample for calibration. A reference sample would optimize reliability and sizing for test under production environment conditions.

Surrogate Fabrication

Surrogates were fabricated using beryllium and bismuth. Bismuth was selected because its longitudinal wave speed and impedance. Bismuth bonded to beryllium creates a high contrast in longitudinal velocity while maintaining a close match in acoustic impedance. Gold and platinum were also considered but were not selected because of their higher velocities, cost, and difficulty in acquiring.

Table 1. Acoustic properties of selected materials

Material	Longitudinal Velocity (km/s)	Acoustic Impedance (MRayl)
Be	12.8	28
Bi	2.1	21

Sample I was constructed using cast bismuth. One drawback of the cast bismuth was that it created relatively large grains (larger than desired), which increases acoustic scattering and attenuation. Higher scattering and attenuation reduces resolution and signal-to-noise of the ultrasound. Sample I was manufactured by bonding beryllium to bismuth with a low viscosity adhesive. Surfaces were prepared by flat lapping and cleaning to ensure a good bond between the materials. Flat-bottom holes of various diameters and depths were machined into the back surface of the bismuth to evaluate detection abilities of the ultrasonic technique. Flaw depths were 0.5 mm, 1 mm, 1.5 mm, and 2 mm. Diameters included 1.5 mm, 3 mm, and 6 mm. Figure 1.1 shows a picture of each sample. A table of the flaw parameters and schematic is given in the Appendix.

Sample II was constructed in the same manner except a commercial bismuth sputtering target was used. In this sample ball-mill type defects of various diameters and sizes were placed in the back surface. These are believed to be more realistic geometries. Depths were 0.5 mm, 1 mm, and 1.5 mm, while the diameters were 1.5 mm, 3 mm, and 6 mm. Figure 1.2 shows a picture of the back surface of the bismuth. A bad area of bismuth was discovered in the ultrasonic tests that results in a large blotch on the scans and is indicated in Figure 1.2.

Figure 1.1 Pictures show top and bottom surfaces of Sample I with flat bottom hole defects on back surface.

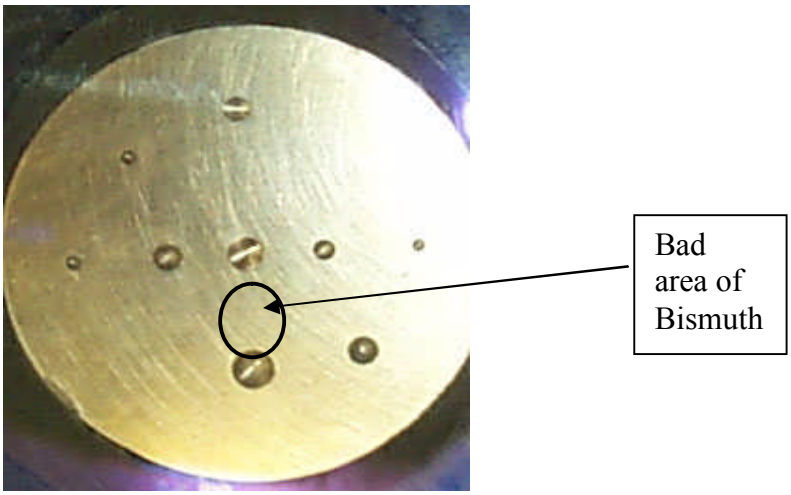

Figure 1.2. A picture of the ball mill defects in Sample II is shown.

Transducer Evaluations

Transducers were evaluated by testing their performance on the surrogate samples and by characterizing them with the reflection from a small steel ball to determine beam patterns, focal point, and sensitivity. Several parameters were analyzed including frequency, element width, focal length, and sensitivity. Transducers from several manufacturers including Panametrics, NDT Systems, and Harisonic were tested. Frequencies ranged from 5 MHz to 30 MHz. Element widths ranged from 6 mm to 12 mm. Focal lengths varied from 25 mm to 50 mm. Piezoceramic and 1-3 piezocomposites were tested.

Sample I and II were tested with this arrangement of transducers and various time-of-flight and amplitude gates were used to image the back surface. 5 MHz was found to be the optimal frequency of operation and was primarily limited by the large grains of bismuth and possibly also limited by the nature of the adhesive bond. In general, the back surface reflection had to be placed outside the gate to obtain quality images. Figure 2.1 shows the time-of-flight images of the back surface of Sample I with a ¼" and ½" diameter transducer. Both transducers were 5 MHz, 1.25" focal length. In this case the ½" transducer gave better results than the ¼" diameter. An RF waveform of a sample A-scan is shown in the Appendix.

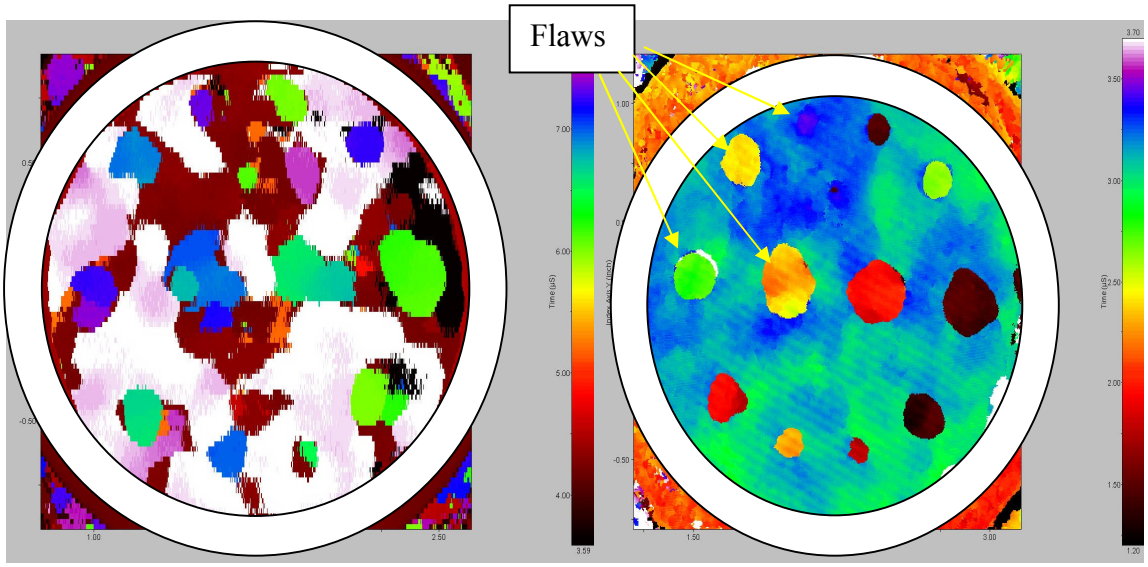

a) b)

Figure 2.1. Images of Sample I show the flat bottom holes with a) ¼" diameter b) ½" diameter transducer.

Next, images were generated using the amplitude of reflection with the back wall reflection outside the gate. Once again, for Sample I the ½" transducer yielded superior results as shown in Figure 2.2. These results show that the ½" aperture is better when dealing with flaws that are planar in nature.

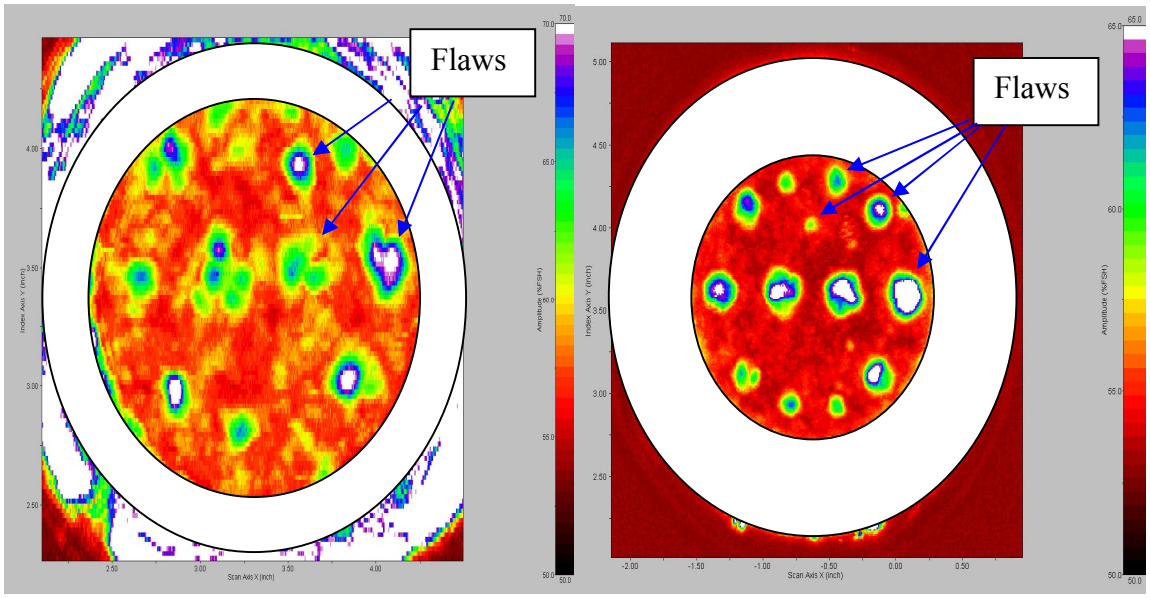

a) b)

Figure 2.2. Images of Sample I were generated using the amplitude of reflection with the back wall outside the gate using a 5 MHz a) ¼" diameter and b) ½" diameter.

Sample II was also evaluated with the same set of transducers. Figure 2.3 shows the images generated using the ¼" and ½" diameter transducers. Both images were generated with amplitude by removing the back surface from the gate. The ½" diameters

transducer has better resolution, but fails to detect some of the smaller flaws. It is still not clear if ¼" or ½" is the better diameter for looking at round-type or other nonplanar flaws.

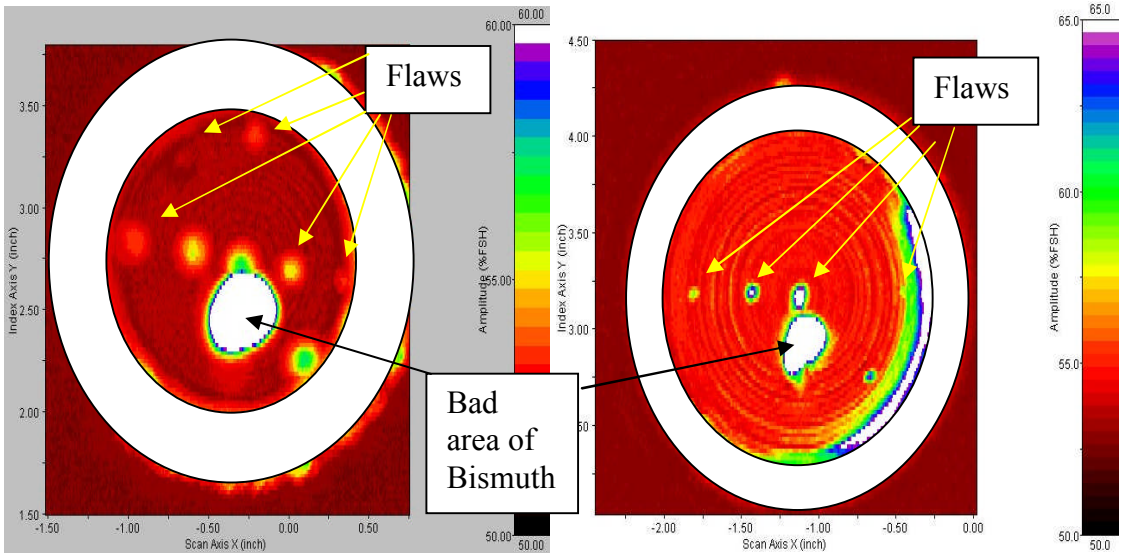

a) ¼" diameter composite transducer b) ½" diameter transducer

Figure 2.3. Images generated of Sample II comparing a) 1/4" diameter and b) ½" diameter transducer.

Squirter Evaluations

Squirters were tested with a gravity flow system. Experiments were conducted at different standoff distances as well as small (4 mm) and large (6 mm) openings. ¼" O.D. tubing with the larger 6 mm opening provided a more laminar flow and improved signal-to-noise of the ultrasound.

Using a larger 6 mm opening squirter yielded much improved images over a smaller 4 mm opening. Figure 3.1a and 3.1b show the images generated for each opening. Data was taken with a 5 MHz NDT System (S/N 065136) ¼" diameter transducer with a standoff distance of 1". Similar results were also obtained for a 5 MHz piezocomposite transducer (S/N 7578). The 6 mm opening produces images with higher contrast and detects all of the ball-mill defects. This is likely because the sound beam has less interference and the water flow is more laminar.

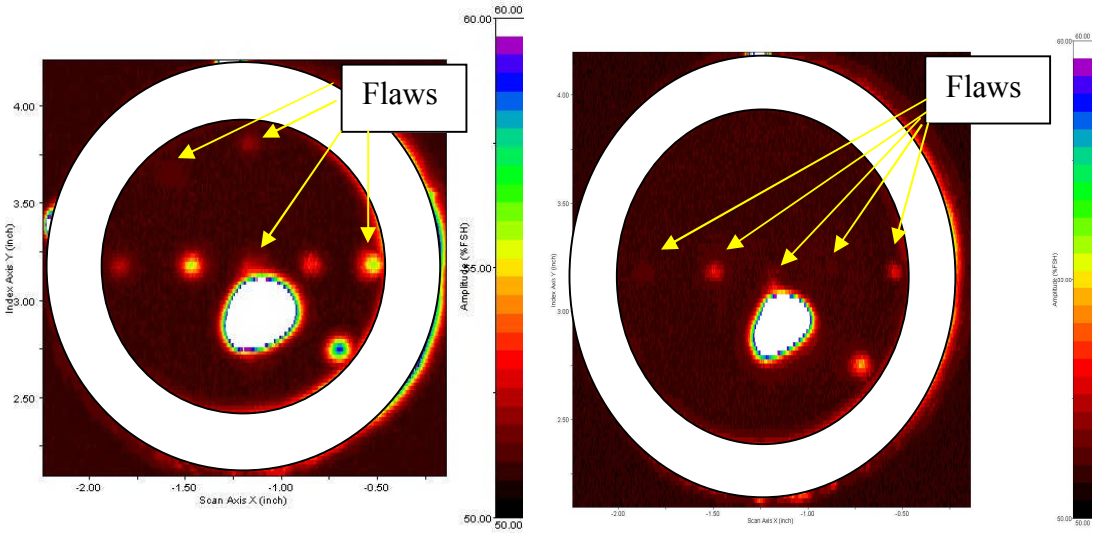

Figure 3.1. a) Image of sample II with 6 mm large transducer opening b) 4 mm small opening

Standoff distance of the transducer was also investigated with the larger and smaller openings. Figure 3.2 shows the image of Sample II generated with a smaller standoff distance of ½". The image has higher contrast and resolution than the image in 3.1a with the longer 1" standoff. This is due to the deeper focus and shorter water path. Similar results were obtained with a smaller opening squirter.

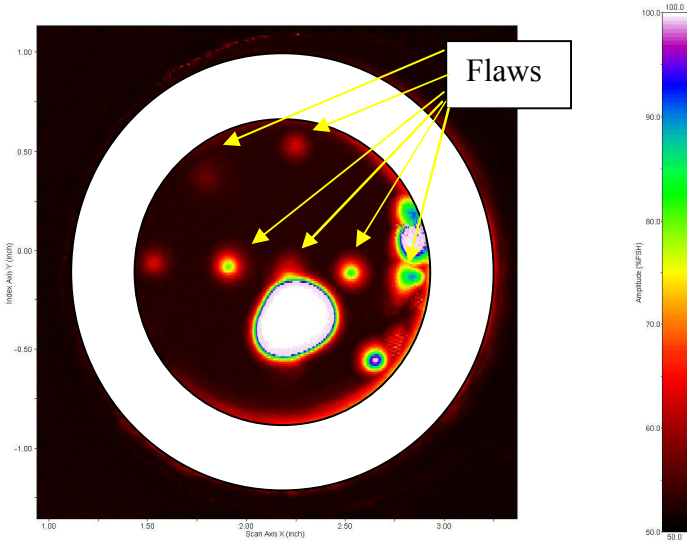

Figure 3.2. Image of Sample II with a 5 MHz ¼" diameter transducer and large opening squirter with a standoff distance of ½".

Transducer Beam Pattern Characterization

Transducers were evaluated using the reflection from a small steel ball. Their beam patterns were evaluated with no squirter, a 4 mm opening squirter, and a 6 mm opening squirter. The beam patterns show that with the 4 mm opening the beam is not as focused or symmetric as is with the 6 mm opening or no squirter at all as shown in Figure 3.3. The experiment shows that the 6 mm opening is sufficient for a ¼" diameter transducer.

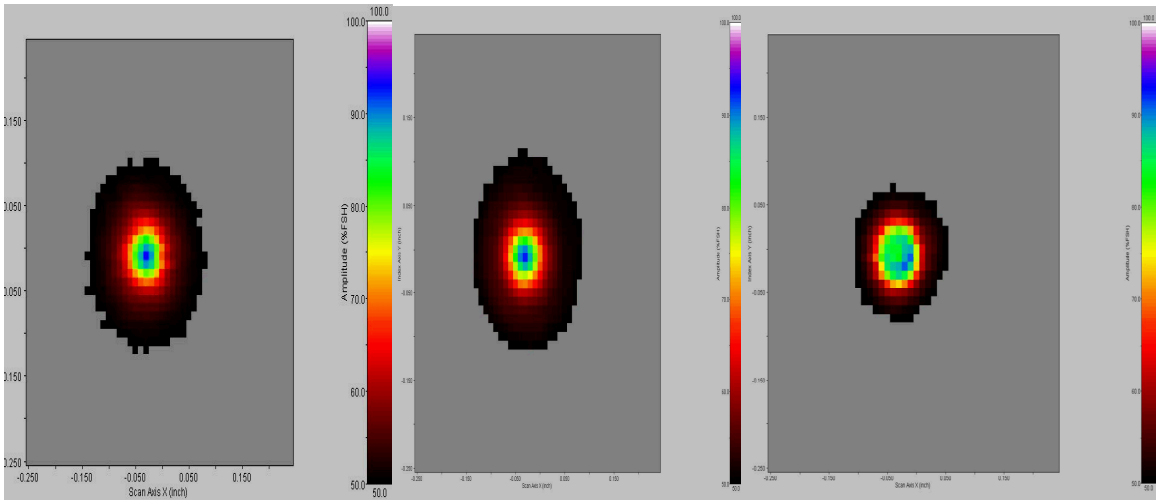

a) b) c)

Figure 3.3. Beam patterns of a 5 MHz ¼" transducer at the focus with a) no squirter b) large 6 mm opening c) small 4 mm opening.

Concluding Remarks

The detection of flat-bottom and ball-mill type defects on the back surface of a Be-Bi structure was demonstrated. Defects as small as 0.5 mm were easily detected. Proper transducer design and gating are critical for detecting and sizing defects that are located at the back surface. Understanding of the nature of the defects (geometry, location, etc.) is critical to establishing the correct gating and feature of the waveform to analyze. Amplitude of the C-scan produced better images for the ball-mill type defects than time-of-flight techniques. 5 MHz, ¼" diameter, 1.25" focus transducers generally provided optimal results. A larger squirter opening enhances resolution and detection abilities. Resolution was improved for the standoff distances of less than ½".

Recommendations

1. Establishment of a reference standard preferably with actual materials with prescribed flaws is highly recommended.
2. Establishment of a transducer characterization facility with a small steel ball reflector would create a method for transducer acceptance and improve understanding of performance.
3. Amplitude features provided better images for evaluating round ball-mill type defects, so amplitude is recommended over time-of-flight.
4. Multiple gates with built-in logic should be used to resolve the back wall reflection from any indications near the back surface.
5. 5 MHz is the recommended frequency for penetration, although 10 MHz should not be ruled out for actual materials.
6. Consider evaluating ½" diameter transducer for actual materials.
7. Tubing and aperture openings on squirters should be widened to ¼" tubing and 3/8" opening to make flow more laminar and create less sound interference.
8. A larger opening bubbler is highly recommended as resolution and detection abilities were significantly improved.
9. Standoff from the transducer to the part was not critical as long as the liftoff of about 1" or smaller and a 1.25" or deeper focal length with a large squirter opening is used. However, resolution was improved for standoff of less than ½".

Appendix

Table 1. Flat-bottom hole parameters of Sample I

Hole No.	Diameter (in.)	Depth (in.)
1	.2508	.0795
2	.2505	.0592
3	.2502	.0390
4	.2505	.0185
5	.1876	.0795
6	.1876	.0584
7	.1871	.0197
8	.1875	.0389
9	.1257	.0589
10	.1251	.0385
11	.1260	.0795
12	.1250	.0192
13	.0628	.0386
14	.0623	.0181
15	.0627	.0588
16	.0620	.0785

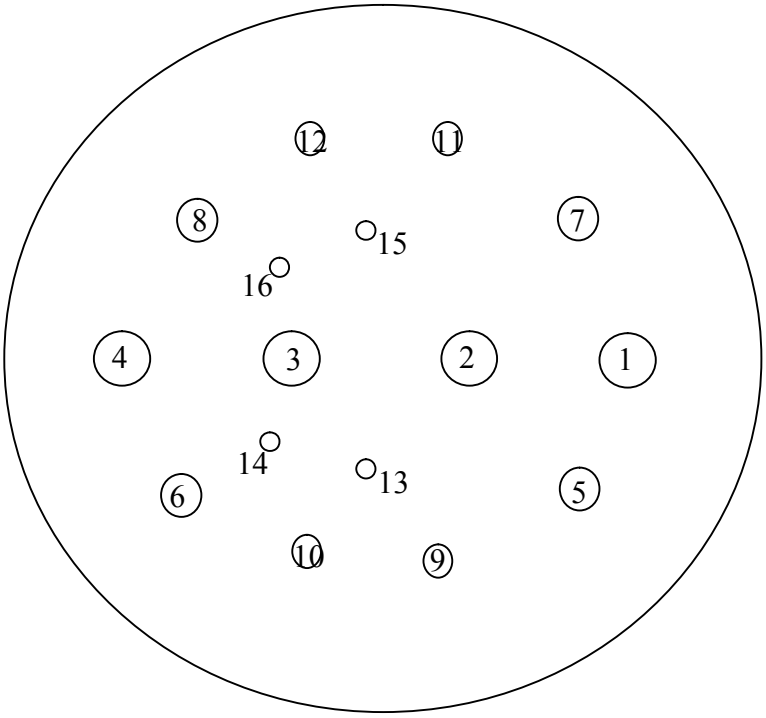

Table 2. Ball-mill defect properties of Sample II

Flaw No.	Diameter (in.)	Depth (in.)
1	0.187	.020
2	0.187	.040
3	0.187	.060
4	0.125	.020
5	0.125	.040
6	0.125	.060
7	0.0625	.020
8	0.0625	.040
9	0.0625	.060

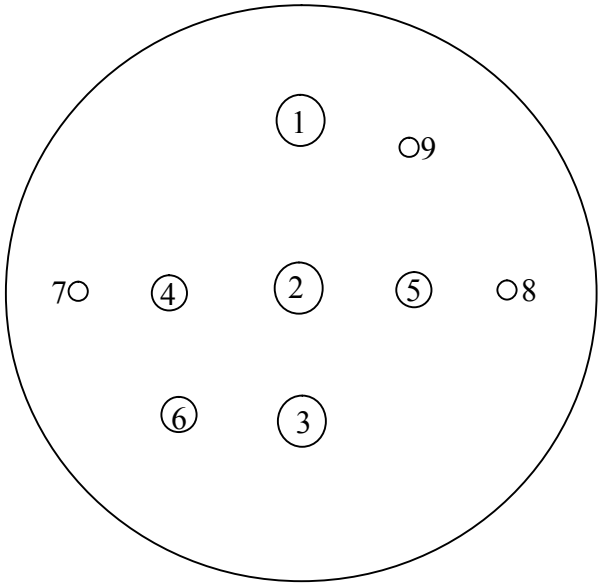

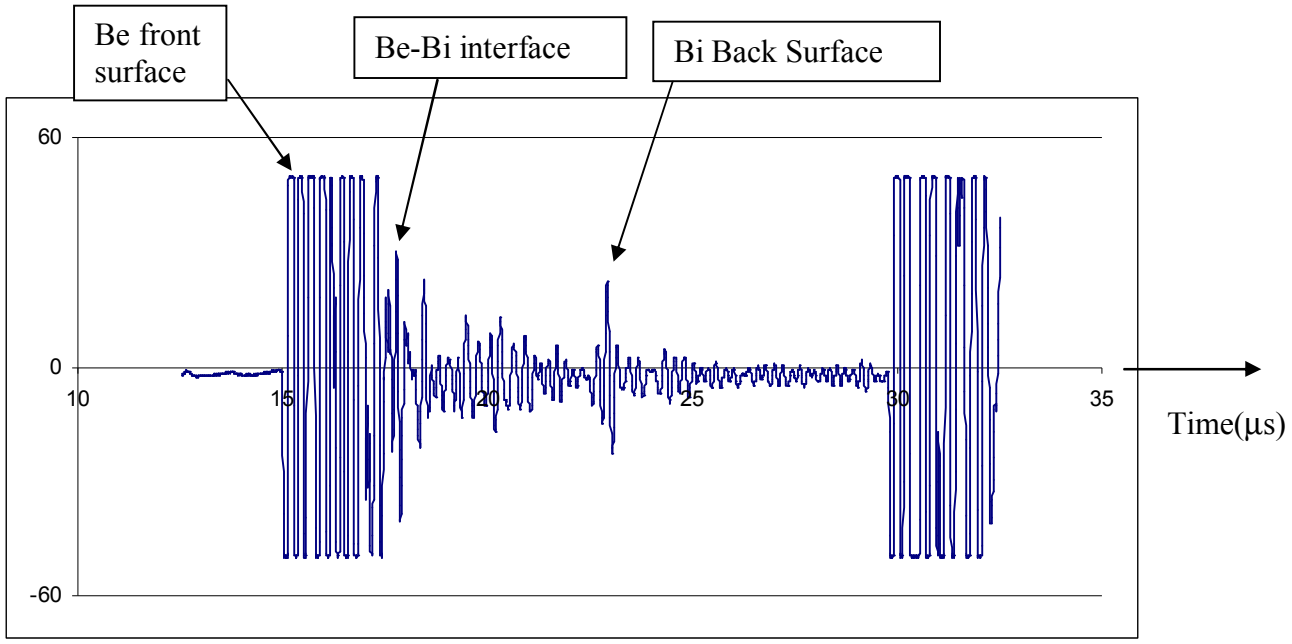

Figure A-1. A sample RF waveform of a Be-Bi sample is shown.